



Providing Choice & Value

Generic CT and MRI Contrast Agents



**FRESENIUS
KABI**

CONTACT REP

AJNR









This information is current as
of July 22, 2025.

**Delayed Enhancement of Intracranial
Atherosclerotic Plaque Can Better
Differentiate Culprit Lesions: A Multiphase
Contrast-Enhanced Vessel Wall MRI Study**

Beibei Sun, Lingling Wang, Xiao Li, Jin Zhang, Jianjian
Zhang, Jiaqi Tian, Mahmud Mossa-Basha, Jianrong Xu, Yan
Zhou, Huilin Zhao and Chengcheng Zhu

AJNR Am J Neuroradiol published online 22 February 2024
<http://www.ajnr.org/content/early/2024/02/22/ajnr.A8132>

Delayed Enhancement of Intracranial Atherosclerotic Plaque Can Better Differentiate Culprit Lesions: A Multiphase Contrast-Enhanced Vessel Wall MRI Study

 Beibei Sun,  Lingling Wang,  Xiao Li,  Jin Zhang, Jianjian Zhang, Jiaqi Tian,  Mahmud Mossa-Basha,  Jianrong Xu, Yan Zhou,  Huilin Zhao, and  Chengcheng Zhu



ABSTRACT

BACKGROUND AND PURPOSE: Intracranial plaque enhancement (IPE) identified by contrast-enhanced vessel wall MR imaging (VW-MR imaging) is an emerging marker of plaque instability related to stroke risk, but there was no standardized timing for postcontrast acquisition. We aim to explore the optimal postcontrast timing by using multiphase contrast-enhanced VW-MR imaging and to test its performance in differentiating culprit and nonculprit lesions.

MATERIALS AND METHODS: Patients with acute ischemic stroke due to intracranial plaque were prospectively recruited to undergo VW-MR imaging with 1 precontrast phase and 4 consecutive postcontrast phases (9 minutes and 13 seconds for each phase). The signal intensity (SI) values of the CSF and intracranial plaque were measured on 1 precontrast and 4 postcontrast phases to determine the intracranial plaque enhancement index (PEI). The dynamic changes of the PEI were compared between culprit and nonculprit plaques on the postcontrast acquisitions.

RESULTS: Thirty patients with acute stroke (aged 59 ± 10 years, 18 [60%] men) with 113 intracranial plaques were included. The average PEI of all intracranial plaques significantly increased (up to 14%) over the 4 phases. There was significantly increased PEI over the 4 phases for culprit plaques (an average increase of 23%), but this was not observed for nonculprit plaques. For differentiating culprit and nonculprit plaques, we observed that the performance of IPE in the second postcontrast phase (cutoff = 0.83, AUC = 0.829 [0.746–0.893]) exhibited superior accuracy when compared with PEI in the first postcontrast phase (cutoff = 0.48; AUC = 0.768 [0.680–0.843]) ($P = .022$).

CONCLUSIONS: A 9-minute delay of postcontrast acquisition can maximize plaque enhancement and better differentiate between culprit and nonculprit plaques. In addition, culprit and nonculprit plaques have different enhancement temporal patterns, which should be evaluated in future studies.

ABBREVIATIONS: AUC = area under the curve; ICC = intraclass correlation coefficient; ICAD = intracranial atherosclerosis disease; IPE = intracranial plaque enhancement; PEI = plaque enhancement index; PI = pituitary infundibulum; ROC = receiver operating characteristic; SD = standard deviation; VW = vessel wall

Intracranial atherosclerosis disease (ICAD) is one of the leading causes of ischemic stroke worldwide.^{1–3} The development of 3D contrast-enhanced vessel wall MR imaging (VW-MR imaging) has improved the evaluation of ICAD by characterizing intracranial plaque features qualitatively and quantitatively.^{4–7} Intracranial

plaque enhancement (IPE), a marker of plaque inflammation, is one of the major high-risk plaque features associated with ischemic stroke.^{8,9} Strong enhancement is associated with recent ischemic events,^{10,11} and it can predict stroke recurrence.^{12–15}

However, there is no standard imaging and analysis method by which to quantify IPE. Most studies evaluated intracranial plaque enhancement via qualitative grading (grade 0: none; grade I: higher than normal wall but less than pituitary infundibulum (PI); grade II: similar to or higher than PI).^{10,16–18} Despite its ease of use by radiologists, qualitative grading lacks quantitative information, and reproducibility (interrater) is only moderate ($\kappa = 0.75$ to

Received May 29, 2023; accepted after revision December 5.

From the Department of Radiology, Ren Ji Hospital (B.S., L.W., X.L., Jin Zhang, Jianjian Zhang, J.T., J.X., Y.Z., H.Z.), and College of Health Science and Technology (B.S., L.W., X.L., Jin Zhang, Jianjian Zhang, J.T., J.X., Y.Z., H.Z.), Shanghai Jiao Tong University School of Medicine, Shanghai, China; and Department of Radiology (M.M., C.Z.), University of Washington, Seattle, Washington.

Beibei Sun and Lingling Wang contributed equally to this work and are co-first authors.

This study was supported by the National Natural Science Foundation of China (grants 82271942, 82171279, 82302181), Science and Technology Commission of Shanghai Municipality Explorer project (22TS400600), Shanghai Municipal Population and Family Planning Commission (20204Y0091), Shanghai Municipal Public Health Excellent Young Talents Training Program (GWVI-II.2-YQ50), and Renji Hospital Shanghai Jiao Tong University School of Medicine (2019NYBSZX01). Chengcheng Zhu was supported by United States National Institute of Health (NIH) grants R01HL162743 and R00HL136883.

Please address correspondence to Huilin Zhao, Department of Radiology, Ren Ji Hospital, Shanghai Jiao Tong University School of Medicine, 160 Pujian Rd, Shanghai 200127, China; e-mail: huilinzhaol2013@163.com

 Indicates article with online supplemental data.

<http://dx.doi.org/10.3174/ajnr.A8132>

0.83).^{10,17,19} Quantitative enhancement is a preferred approach and has been used in many recent studies.^{20–23} Additionally, in previous studies, the timing of postcontrast VW-MR imaging after contrast injection either varied, ranging from 0 to 20 minutes,^{10,13,24–26} or was unreported.²⁷ A dynamic enhancement study indicated that intracranial atherosclerosis enhancement might change over time.²⁸ Thus, it is important to optimize the timing to maximize lesion enhancement for the identification of high-risk lesions and to standardize the protocol for future multicenter studies.

The purposes of this study are as follows: 1) identify the ideal postcontrast timing for enhancing the visualization of IPE by using multiphase contrast-enhanced VW-MR imaging and 2) explore the suitable postcontrast timing for distinguishing between culprit and nonculprit lesions.

MATERIALS AND METHODS

Study Population

Informed consent was obtained from all participants, and all protocols were approved by the institutional review board. Consecutive patients with acute ischemic stroke (within 4 weeks of symptoms) due to intracranial atherosclerotic plaque were prospectively recruited between March 2020 and March 2021, and they underwent full-head 3D contrast-enhanced VW-MR imaging. The inclusion criteria for this study were: 1) patients with intracranial arterial stenosis detected on MR angiography, CT angiography, or digital subtraction angiography; 2) ischemic infarct confirmed by DWI within 4 weeks; and 3) stroke etiology determined to be intracranial artery stenosis via the identification of intracranial artery plaque on 3D VW-MR imaging. The exclusion criteria were: 1) intracranial artery occlusion; 2) a high risk of carotid artery-to-artery embolism: the coexistence of >50% stenosis or unstable plaques (the presence of at least 3 of the following features: calcification, hemorrhage, superficial irregularity, and being lipid-rich) of the ipsilateral extracranial carotid artery having been detected via imaging (sonography, MR angiography, CT angiography, or digital subtraction angiography); 3) complex aortic arch plaques confirmed by CT angiography (plaque with complex composition or ulcerated or thickness ≥ 4 mm)²⁹; 4) evidence of cardioembolic source ischemic stroke (recent myocardial infarction within 3 weeks, atrial fibrillation or flutter, evidence of cardiac or valvular thrombus on echocardiography or other imaging); 5) clinical evidence of the presence of vasculopathy, other than atherosclerosis (eg, vasculitis, reversible cerebral vasoconstriction syndrome, or other vasospastic processes, Moyamoya disease, or dissection); 6) degraded image quality of 3D VW-MR imaging that limited the accurate delineation of the artery boundaries for quantitative analysis; and 7) subsequent scans were abandoned if any stage of the postcontrast phases had an unsatisfactory image quality. Participants' data, including vascular risk factors such as age, sex, body mass index, hypertension, diabetes, dyslipidemia, and current smoking, were extracted from an institutional database.

3D VW-MR Imaging Protocol

VW-MR imaging was performed on a 3T MR scanner (Prisma, Siemens) by using a 64-channel phased-array neurovascular coil. The imaging protocol included 3D time-of-flight MR angiography

as well as 1 precontrast and 4 postcontrast enhanced T1-weighted 3D sampling perfection with application-optimized contrasts by using different flip-angle evolutions (SPACE; Siemens) acquisitions. The 3D time-of-flight MR angiography used the following parameters: TR/TE, 21.0/3.69 ms; number of slices, 48; flip angle, 16°; field of view, 220 × 195 mm²; voxel size, 0.6 mm³; acquisition matrix, 384 × 345; slabs, 5; and scan time, 6 minutes and 2 seconds. This was followed by precontrast T1-weighted SPACE with the following parameters: sagittal imaging orientation; TR/TE, 1000/15 ms; number of slices, 240; field of view, 193 × 193 mm²; voxel size, 0.6 mm³; acquisition matrix, 320 × 320; slabs, 1; and scan time, 9 minutes and 13 seconds. Motion-sensitized driven equilibrium was used to suppress the signal of slow flow with a 500 mTms²/m gradient in the x-y-z directions in order to enhance the visualization of the vessel wall.³⁰ Four consecutive phases of postcontrast T1-SPACE were acquired after a gadolinium-based contrast (Magnevist) injection (0.1 mmol/kg at a rate of 1.5 mL/s). Four postcontrast phases were consecutively scanned immediately after the injection of the contrast agent without any time intervals in between. These phases were initiated at the following time intervals after the contrast injection: 0 minutes for the first phase, 9 minutes and 13 seconds for the second phase, 18 minutes and 26 seconds for the third phase, and 27 minutes and 39 seconds for the fourth phase. The total scan time of the 4 postcontrast phases was 36 minutes and 52 seconds.

Image Analysis

Three neuroradiologists (B.S., L.W., and X.L., each with 6 years of experience in neurovascular imaging), blinded to clinical information, each independently reviewed VW-MR imaging studies on PACS software (Carestream Health, Version 11.4.0.0179), and performed qualitative and quantitative measurements. Discrepancies were resolved through a consensus discussion with a fourth radiologist (H.Z., with 12 years of experience in neurovascular imaging). An image quality rating was assigned by using a 3-point scale, where 1 = poor [low SNR and obscured vessel wall or lumen boundaries], 2 = marginal (passable SNR with a few motions or blood artifacts, distinguishable vessel wall, but partially obscured vessel lumen and wall boundaries), and 3 = good (high SNR without artifacts, clearly displaying vessel lumen boundary and wall).³¹ The MR data sets with image quality ratings of 1 were excluded from further analyses. Intracranial atherosclerotic plaques were identified by using a previously reported definition (the presence of focal wall thickening¹⁰ on both precontrast and postcontrast VW-MR imaging. The raters identified all plaques involving the arterial branches of the circle of Willis, including the C4–7 segment of the internal carotid artery, the A1–2 segment of the anterior cerebral artery, the M1–2 segment of the middle cerebral artery, the V4 segment of the vertebral artery, the P1–2 segment of the posterior cerebral artery, and the basilar artery.

The culprit plaque was defined as 1) the only lesion within the vascular territory of the stroke or 2) the most stenotic lesion when multiple plaques were present upstream of the stroke territory.¹⁰ We have identified a total of 30 culprit plaques, with 24 falling into category A (representing the sole lesion within the

vascular territory of the stroke) and 6 falling into the less common category B (in which multiple plaques were present upstream of the stroke territory). For these 6 category B plaques, detailed information on their location, enhancement grade, and stenosis grade are provided in the Online Supplemental Data. All 6 of the category B culprit plaques have the highest stenosis degree as well as the highest enhancement degree. There was no plaque that had a high enhancement but a low degree of stenosis. In addition, we have excluded patients presenting with the scenario in which the most stenotic plaque exhibits lower enhancement and a less stenotic plaque displays strong enhancement, as this situation can pose challenges in defining the culprit plaque.

The plaque enhancement grade was classified into 3 grades on the postcontrast T1-SPACE images by using previously published criteria:^{10,32} grade 0, no enhancement, defined as the signal intensity of the plaque being similar to that of the adjacent normal vessel wall; grade I, mild enhancement, defined as the signal intensity of the plaque being lower than that of the pituitary infundibulum but higher than that of the adjacent normal vessel wall; and grade II, obvious enhancement, defined as the signal intensity of the plaque being similar to or greater than that of the pituitary infundibulum. Though a quantitative analysis method is preferred to qualitative grading, we still performed grading in this study to identify the potential changes of grades when the postcontrast scans were acquired at different times, and such grading was widely used in previous clinical studies.

Quantitative plaque enhancement was analyzed by using the plaque enhancement index (PEI).

$$PEI = \frac{\frac{SI_{\text{plaque-post}}}{SI_{\text{CSF-post}}} - \frac{SI_{\text{plaque-pre}}}{SI_{\text{CSF-pre}}}}{\frac{SI_{\text{plaque-pre}}}{SI_{\text{CSF-pre}}}}$$

where “pre” indicates precontrast enhanced images and “post” indicates postcontrast enhanced images. The SI of plaque was measured on a section orthogonal to the course of the parent artery with images that were magnified 6-fold on the image viewer. Three ROIs were placed over the target lesion, on the section with the most conspicuous lesion enhancement and on the adjacent section in each direction on the first postcontrast phase images. The PEI was calculated by the mean SI of the ROIs from the 3 slices. The reference structure CSF expected to normalize PEI was also measured (an ROI of 10 mm² drawn on the frontal horn of the right lateral ventricle). It needs to be mentioned that few patients changed position during the scanning process. So, we did not register the precontrast and 4 phases of postcontrast images in the same patient, but the measurement of the ROIs of the reference object and plaque was copied between the precontrast and 4 phases of postcontrast images (automatic align). Then, the position was manually adjusted, which ensured that the ROIs’ positions and sizes in the pre contrast and 4 phases of postcontrast images were consistent. The ROI of the intracranial plaque and CSF were all manually segmented by using medical imaging viewer software (Vue PACS Livewire, Carestream).

Within this study cohort, 20 plaques (10 culprit plaques and 10 nonculprit plaques) in 10 cases were randomly selected. A

quantitative analysis was independently performed by 2 radiologists (B.S. and L.W., each with 6 years of experience in neurovascular imaging). A qualitative analysis was performed by 3 radiologists (B.S., L.W., and X.L., each with 6 years of experience in neurovascular imaging). One reviewer (L.W.) independently reevaluated the same 20 plaques 2 months after the initial evaluation for an intrarater agreement analysis.

Statistics

All analyses were performed by using the SPSS software package (version 23.0). Continuous data are presented as mean \pm standard deviation (SD). All variables were tested for normal and homogeneous variance by using the Shapiro-Wilk normality test and Levene test, respectively. Categorical variables were recorded as frequencies and percentages. Multiple paired *t* tests were conducted after a 1-way repeated-measures ANOVA to assess differences among the 4 postcontrast phases. To address the issue of multiple comparisons and the nonindependence of plaques within the same subjects, we first applied the Bonferroni correction to control the family error rate and maintain overall significance levels. Second, to account for the nonindependence of plaques within the same subjects, we utilized a mixed-effects model repeated measures ANOVA for multiple comparisons. Interobserver and intraobserver agreement were calculated with the Kendall W or Cohen κ value for the categorical data and the intraclass correlation coefficient (ICC) for the continuous data. A value of Kendall W, Cohen κ or ICC of >0.80 indicated excellent agreement. All tests were 2-tailed, and *P* values of $<.05$ were considered to be indicative of a statistically significant result. A 1-way repeated measures design with a sample of 60 subjects (30 patients for each group), measured at 4 time points, achieved a 0.15 effect size and 95% power to detect differences among the PEI means by using a Geisser-Greenhouse corrected *F* test at a .05 significance level. The standard deviation across subjects at the same time point was assumed to be 0.515. The pattern of the covariance matrix is to have all correlations equal with a correlation of 0.7 between the first and second time point PEI measurements. These calculations were conducted by using PASS 2023 Power Analysis and Sample Size Software (2023) (NCSS). The result showed that a minimum sample size of 30 was needed in each group. Accordingly, we planned to include 30 participants in this prospective study. The receiver-operating characteristic (ROC) curves to differentiate between culprit and nonculprit lesions were plotted for 4 postcontrast phases, and the area under the curve (AUC) values were calculated. We utilized the DeLong test to compare the ROC curves between postcontrast phases. This test calculates a test statistic (*z*) and its corresponding *P* value based on paired ROC curves and the standardized area differences between them. Additionally, to determine the optimal cutoff value used to estimate sensitivity and specificity, we conducted a comprehensive analysis by maximizing the Youden index derived from the ROC curve.

RESULTS

Patient Demographics and Intracranial Plaque Characteristics

From March 2020 to March 2021, 62 participants were recruited to undergo 3D VW-MR imaging. Thirty-two participants were

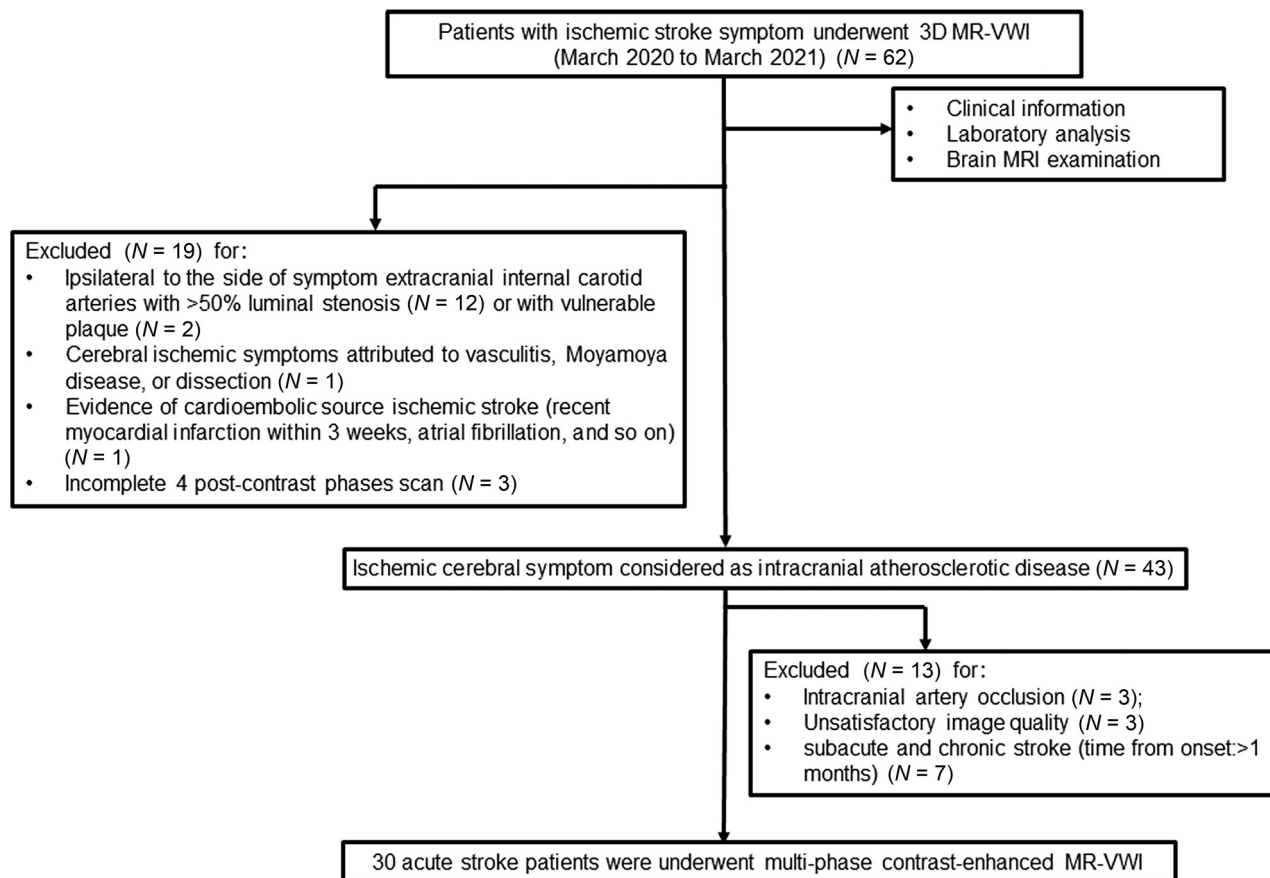


FIG 1. Patient selection flow chart.

Table 1: Demographic and intracranial plaque characteristics of 30 patients with acute stroke

Patient Demographics	Mean \pm SD or Median (IQR) or n (%)
Age (years)	59.0 \pm 9.7
Body mass index (kg/cm ²)	24.6 \pm 2.9
Sex (male)	18 (60.0%)
Hypertension	21 (70.0%)
Diabetes	11 (36.7%)
Dyslipidemia	6 (20.0%)
Current smoking	5 (16.7%)
Plaque location	
Internal carotid artery (C4–7)	25 (22.1%)
Middle cerebral artery	34 (30.1%)
Anterior cerebral artery	6 (5.3%)
Basilar artery	17 (15.0%)
Vertebral artery	21 (18.6%)
Posterior cerebral artery	10 (8.9%)
Plaque stenosis (%)	
30% \leq stenosis < 50% (grade I)	74 (65.5%)
50% \leq stenosis < 70% (grade II)	15 (13.3%)
Stenosis \geq 70% (grade III)	24 (21.2%)
Plaque numbers (n)	3.0 (2.0–6.0)

excluded because of 1) intracranial artery occlusion ($n = 3$); 2) the coexistence of ipsilateral extracranial carotid atherosclerosis with $>50\%$ stenosis ($n = 12$) or unstable features ($n = 2$); 3) evidence of cardioembolic source ischemic stroke ($n = 1$); 4) the presence of nonatherosclerotic intracranial vasculopathy ($n = 1$); 5) insufficient image quality ($n = 3$); 6) a stroke >1 month since

onset ($n = 7$); and 7) having an incomplete set of 4 postcontrast phase scans ($n = 3$). The flow chart is summarized in Fig 1. Finally, a total of 30 patients with 113 plaques were included (aged 59 ± 10 years, 18 [60.0%] men). The median plaque number for the group of patients is 3.0 [interquartile range, [2.0–6.0]]. The demographic and intracranial plaque characteristics are summarized in Table 1.

Dynamic Changes of Quantitative Enhancement of Culprit and Nonculprit Plaques

The PEI of all intracranial plaques significantly increased (on average 14.1%) over time after the contrast injection, from 0.64 ± 0.49 at the first postcontrast phase to 0.73 ± 0.51 at the fourth postcontrast phase ($P = .033$). For the culprit plaque, the PEI significantly increased 22.1% with time after the contrast injection, from 1.02 ± 0.53 at the first postcontrast phase to 1.20 ± 0.49 at the fourth postcontrast phase ($P = .034$). There were no significant differences between the second and third, second and fourth, or third and fourth postcontrast phases in either the all intracranial plaques or the culprit plaques. In addition, the nonculprit plaques showed no significant differences among the 4 postcontrast phases ($P = .450$) (Fig 2 and Table 2). Two examples of patients with culprit and nonculprit plaques are demonstrated in Fig 3.

The ROC curves for distinguishing between culprit and nonculprit plaques are graphically represented in Fig 4, and a detailed summary of the AUC values can be found in Table 3. Specifically,

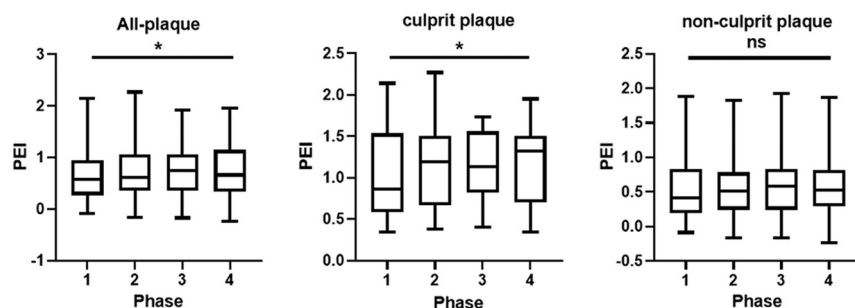


FIG 2. Plaque enhancement index (PEI; the mean signal intensity of plaque normalized by CSF) change of culprit and nonculprit plaques over time. The boxes were drawn with the median (*line in the box*) as well as the 25th and 75th percentiles. The bars above and below the box are the maximum and minimum values of the PEI, respectively. The PEI values of all intracranial plaques and culprit plaques increase over the 4 phases ($P = .033$, $P = .034$, respectively). The PEI values of the nonculprit plaques show no significant differences among the 4 postcontrast phases ($P = .450$). *, $P < .05$; ns, not significant.

Table 2: Plaque enhancement index change of culprit and nonculprit plaques over time

Phase	PEI		
	All Plaques (n = 113) ^a	Nonculprit Plaque (n = 83) ^a	Culprit Plaque (n = 30) ^b
1st	0.66 ± 0.51	0.54 ± 0.44	1.02 ± 0.53
2nd	0.72 ± 0.52	0.55 ± 0.42	1.17 ± 0.50
3rd	0.73 ± 0.47	0.58 ± 0.39	1.16 ± 0.41
4th	0.76 ± 0.53	0.60 ± 0.44	1.20 ± 0.49
P^c	.033	.450	.034
P 1st versus 2nd	.014	.578	.007
P 1st versus 3rd	.049	.446	.057
P 1st versus 4th	.029	.401	.035
P 2nd versus 3rd	.879	.640	.869
P 2nd versus 4th	.502	.572	.680
P 3rd versus 4th	.458	.771	.477

^a A mixed-effects model repeated measures ANOVA for continuous variables was used to analyze the differences between all 4 postcontrast phases in all plaque groups and the nonculprit plaque group.

^b A 1-way repeated-measures ANOVA for continuous variables was used to analyze the differences between the 4 postcontrast phases in the culprit plaque group. This was followed by a pair-wise comparison post hoc analysis using Bonferroni correction to compare the differences between the PEI values of each 2 contrast phases.

^c P values of the comparisons of the 4 postcontrast phases.

the AUC values for PEI in the 4 postcontrast phases were 0.768 (0.680–0.843), 0.829 (0.746–0.893), 0.840 (0.759–0.902), and 0.812 (0.727–0.879), respectively.

The cutoff values of PEI in the 4 postcontrast phases were 0.48 (sensitivity = 59.0%, specificity = 86.7%), 0.83 (sensitivity = 80.7%, specificity = 70.0%), 0.95 (sensitivity = 83.1%, specificity = 70.0%), and 0.98 (sensitivity = 84.3%, specificity = 70.0%), respectively. In addition, the AUC for PEI in the second postcontrast phases was higher than that observed for PEI in the first postcontrast phases ($P = .022$) to detect culprit plaques, but no differences were found between the other postcontrast phases (Table 4).

Dynamic Changes of Qualitative Enhancement of Culprit and Nonculprit Plaques

As shown in the Online Supplemental Data, during the 4 postcontrast enhanced phases, the grade II percentage of culprit plaques was higher than that of the nonculprit plaques, and the grade 0 and grade I percentages of culprit plaques were both lower than those of the nonculprit plaques. As shown in the first postcontrast phase, there were 16 (14.2%)

grade 0, 69 (61.1%) grade I, and 28 (24.7%) grade II plaques. Over time, the degree of enhancement increased over subsequent phases. The grade II plaques significantly increased from 28 (24.7%) to 54 (47.8%) ($P < .05$), whereas the grade 0 (from 14.2% to 6.2%) and grade I (from 61.1% to 46.0%) plaques showed a decreasing trend ($P > .05$). In addition, the enhancement grade changed a lot during the 4 postcontrast enhanced phases in the culprit and nonculprit plaques ($P = .020$ and $P = .006$, respectively). The percentage of grade II tended to increase during the 4 postcontrast enhanced phases in the culprit and nonculprit plaques, whereas the percentages of grade I and grade 0 gradually decreased during the 4 postcontrast enhanced phases.

The enhancement grades of 42 (37.2%) plaques in 17 (56.7%) patients changed during the 4 postcontrast phases (Online Supplemental Data). 30% of the culprit plaques from 9 patients showed an enhancement grade change from grade I to grade II. Similarly, in the nonculprit plaque group, 39.8% of the plaques from 18 patients exhibited an enhancement grade change.

The ability of the enhancement grade to differentiate between culprit and nonculprit plaques did not show a

significant difference among the 4 postcontrast enhanced phases (Online Supplemental Data).

3D VW-MR Imaging Measurement Reproducibility

The interrater and intrarater reproducibility data are summarized in the Online Supplemental Data. There was excellent interrater and intrarater agreement for all measurements (all Kendall κ and ICC values were greater than 0.80).

DISCUSSION

In this study, we attempt to standardize the postcontrast timing for evaluating intracranial vessel wall enhancement by using multiphase contrast-enhanced VW-MR imaging. We found that 1) a 9-minute delay in postcontrast acquisition proved to be beneficial for enhancing plaque visibility and enhancing the differentiation between culprit and nonculprit plaques and 2) culprit and nonculprit plaques exhibit unique enhancement patterns over time, which is a facet deserving of exploration in future research. Such results highlight the importance of the standardization of imaging protocols and possibly explain the large variability of previous studies due to inconsistent postcontrast timing. Our study

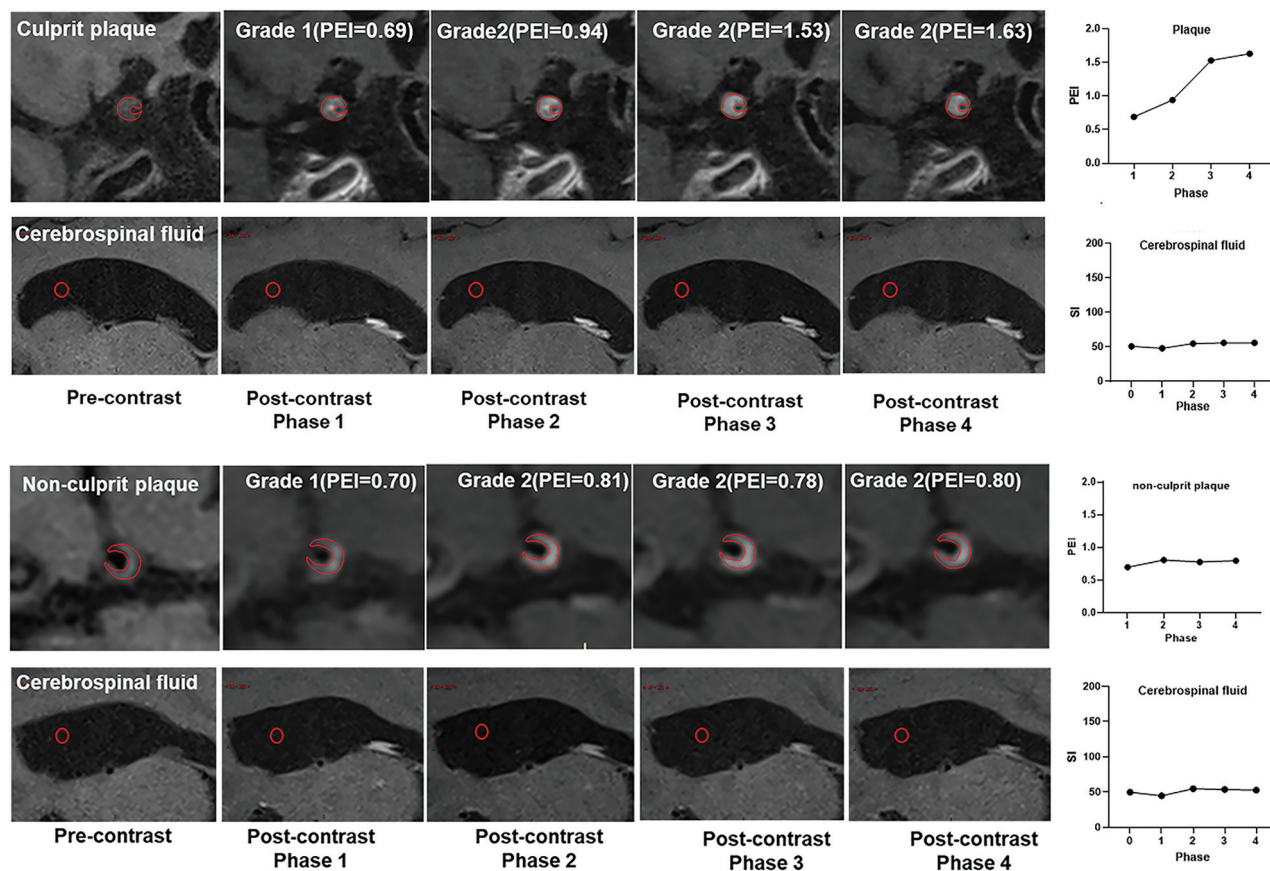


FIG 3. Cases of the culprit and nonculprit plaque signal intensity change during the 4 postcontrast phases.

provides an important reference for the design of future multicenter studies targeting intracranial plaques on VW-MR imaging and stroke risk. The 9-minute delay could also be considered for utilization in other postcontrast sequences as a part of the clinical stroke imaging protocol, potentially without extending the overall duration of the MR imaging examination.

The time interval of postcontrast VW-MR imaging after contrast administration was inconsistent in previous studies, ranging from 0–20 minutes (or was unreported in many studies). Skarpathiotakis et al²⁶ obtained postcontrast images immediately after contrast administration, whereas Qiao et al¹⁰ acquired postcontrast images 5 minutes after contrast injection. Song et al¹³ obtained postcontrast images within 10 minutes after the administration of contrast injection, whereas Vakil et al²⁵ performed postcontrast T1-weighted imaging within 20 minutes of contrast injection. Because of the large variation of these previous studies, the enhancement measurements were not interchangeable. De Havenon et al³³ retrospectively examined the impact of time intervals between contrast administration and postcontrast VW-MR imaging (range from 0 to 40 min) on the enhancement of 35 intracranial plaques in 35 patients with acute ischemic stroke and found that a longer duration after contrast injection was associated with increased plaque enhancement. However, each patient had only 1 postcontrast acquisition with variable postcontrast timing, and the effects of interpatient differences could not be ruled out. Stroke severity, stroke acuity at the time of imaging, and other factors could lead to different plaque enhancement.

Our prospective study had a more rigorous design through the use of Multiphase postcontrast VW-MR imaging in the same patient.

Our study also found that by prolonging the time interval between contrast administration and postcontrast VW-MR imaging to at least 9 minutes, the plaque enhancement index increased. After the injection of the gadolinium contrast agent, the contrast goes into the plaque in one of two possible ways: 1) via the vasa vasorum⁹ (neovasculture) in the adventitia of the artery and 2) via direct penetration from the surface of the plaque. By either way, it needs a few minutes or longer to reach the peak concentration. Such a phenomenon is also present in other diseases. For example, in cardiac MR imaging examinations, late gadolinium enhancement is widely used to detect myocardium scars. Delayed contrast-enhanced scans with CT or MR are also the standard clinical imaging protocol for adrenal glands and tumors.³⁴ We also noticed that increasing the delay time to 18 minutes or longer will not further increase the enhancement. Thus, the delay of 9 minutes is the best option without excessively increasing the scan time. We also found that delayed enhancement could better distinguish between culprit and nonculprit plaques. This was because the culprit plaques had different enhancement curves than did the nonculprit plaques. The culprit plaques had increased PEI levels and then stayed at a high PEI level. The nonculprit plaques did not have a significant increase in PEI, even when acquired with a long delay. The reason may be that culprit plaques had rich vasa vasorum and high permeability,

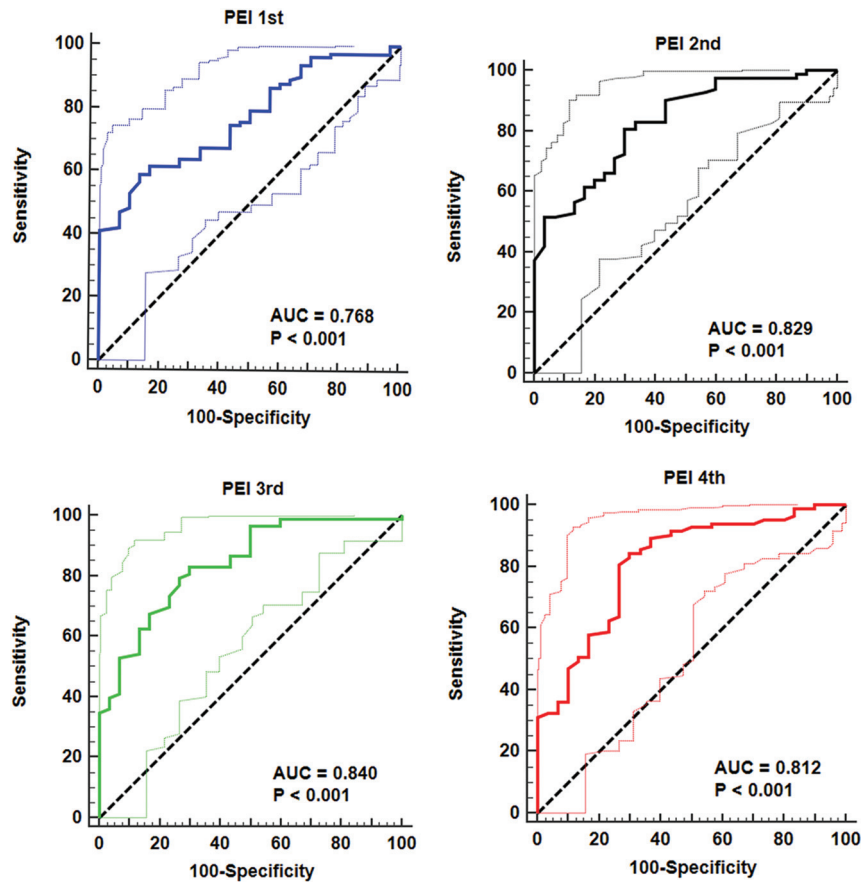


FIG 4. The ROC of the plaque enhancement index in the 4 contrast-enhanced phases for differentiating between culprit and nonculprit plaques.

Table 3: Plaque enhancement index in different contrast-enhanced phases to differentiate between culprit and nonculprit plaques

Variables	AUC (95% CI)	Sensitivity/Specificity	Cutoff	P Value
PEI 1st	0.768 (0.680–0.843)	59.0%/86.7%	0.48	<.001
PEI 2nd	0.829 (0.746–0.893)	80.7%/70.0%	0.83	<.001
PEI 3rd	0.840 (0.759–0.902)	83.1%/70.0%	0.95	<.001
PEI 4th	0.812 (0.727–0.879)	84.3%/70.0%	0.98	<.001

Table 4: Comparison of ROC curves of PEI to differentiate between culprit and nonculprit plaques between 4 postcontrast phases

Variables	Difference between AUC area	95% CI	z statistic	P Value
PEI 1st versus PEI 2nd	0.060 ± 0.026	0.009–0.112	2.293	.022
PEI 1st versus PEI 3rd	0.071 ± 0.039	–0.005–0.148	1.824	.068
PEI 1st versus PEI 4th	0.043 ± 0.038	–0.032–0.118	1.131	.258
PEI 2nd versus PEI 3rd	0.011 ± 0.025	–0.038–0.060	0.444	.657
PEI 2nd versus PEI 4th	0.017 ± 0.027	–0.036–0.070	0.628	.530
PEI 3rd versus PEI 4th	0.028 ± 0.024	–0.020–0.076	1.151	.249

whereas the nonculprit plaques lacked such high-risk features. It is noteworthy that researchers such as Qiao et al¹⁰ have successfully employed a 5-minute delay in their studies, as exemplified in their work published in *Radiology*. This raises the possibility that a 5-minute delay might be adequate for distinguishing between culprit and nonculprit plaques. It is essential to highlight that the main focus of our study was not only to distinguish between plaque types but also to understand how intracranial plaque enhancement changes over time. The 9-minute delay recommended in clinical practice may not be realistic. The need for dynamic contrast-enhanced scans²⁸ with high temporal

resolution is recognized to guide us toward achieving better results with shorter delay times. However, the study design involves longitudinal/multiphase postcontrast acquisition in the same patient, and the findings above suggest that our study remains relevant. Our study serves as an initial exploration of a trend, albeit within a small sample. It underscores the need for further research with larger sample sizes and an improved study design to complement and refine these initial findings.

In addition, we observed significant changes in the enhancement grade between culprit and nonculprit plaques at 4 enhancement periods, with 42 (37.2%) plaques in 17 (56.7%)

patients displaying changes during the 4 postcontrast phases (Online Supplemental Data). The enhancement grade of 30% of the culprit plaques in 9 patients changed from grade I to grade II. Similarly, in the nonculprit plaque group, 39.8% of plaques from 18 patients showed enhanced grade changes. Our findings demonstrated that the enhancement grade is not fixed but dynamically changing, with some grade I plaques transitioning to grade II and vice versa over time. The possible reason for the above phenomenon is that the pituitary infundibulum (the reference used to assess enhancement grade) also changes over time. We have also found that there is no statistically significant difference in the differentiation ability of enhancement grades between culprit and nonculprit plaques across the 4 postcontrast phases. These findings suggest that enhancement grades alone may not provide a strong discriminatory capability to distinguish between these plaque types. Different from our study, Kwee et al³⁵ investigated intracranial atherosclerotic plaques in patients at 140 days poststroke and found differences in the evolution of culprit and nonculprit plaques. They demonstrated that the contrast enhancement grade of intracranial atherosclerotic plaques can persist for months after an ischemic event. The culprit plaques showed the highest baseline enhancement grade more frequently and were more likely to remain at grade II, whereas the nonculprit plaques were more likely to show a decline in enhancement grade at follow-up.

In our study, we focused on determining the optimal postcontrast timing for differentiating between culprit and nonculprit plaques. We conducted longitudinal/multiphase postcontrast vessel wall MR imaging to evaluate how the enhancement of intracranial plaques changes over time within relatively shorter imaging intervals (0, 9, 18, and 27 minutes after the contrast injection). Our findings are based on a different approach that is aimed at understanding how plaque enhancement changes in acute ischemic stroke phases (within 4 weeks of symptoms) following contrast administration. Kwee et al's³⁵ study examined patients at a much later time point (140 days poststroke) and offered insights into the plaque changes that occur in the post-stroke period, shedding light on the longer-term implications. In contrast, our study aimed to determine the optimal timing for clinical imaging in the acute phase, which has value in the diagnosis and management of patients with acute ischemic stroke. We provided insights into an early dynamic of plaque enhancement, specifically within an hour of contrast injection. The above findings suggest that the enhancement effects vary at different periods. Further validation in chronic patients is needed.

This study had several limitations. First, the 9-minute delay used in our study may not be realistic in clinical practice. As imaging technology advances, shorter scan times can provide more detailed temporal resolution, which is crucial for capturing subtle changes in plaque enhancement. Second, this was a single-center study that used only 1 scan protocol (3D SPACE) with 1 vendor (Siemens) and 1 contrast agent (Magnevist at 0.1 mmol/kg). Multicenter studies across multiple scan protocols and multiple platforms will be needed to confirm our results. Third, the difference in enhancement behavior between culprit and nonculprit plaques may depend on the arterial input (which may vary between subjects). However, postcontrast

images were acquired a few minutes after the injection (about 9 minutes). By this time, the contrast agent has been evenly distributed into the blood. Finally, our study has a limited sample size, and some nonculprit plaques came from the same patients. To ensure robust and unbiased statistics, we used correction methods. A larger-scale study is needed to validate the findings and extend the current research.

CONCLUSIONS

A 9-minute delay of postcontrast acquisition can maximize plaque enhancement and better differentiate between culprit and nonculprit plaques. In addition, culprit and nonculprit plaques have different enhancement temporal patterns, which should be evaluated in future studies.

Disclosure forms provided by the authors are available with the full text and PDF of this article at www.ajnr.org.

REFERENCES

1. Arenillas JF. **Intracranial atherosclerosis: current concepts.** *Stroke* 2011;42:S20–3 [CrossRef Medline](#)
2. White H, Boden-Albala B, Wang C, et al. **Ischemic stroke subtype incidence among whites, blacks, and Hispanics: the Northern Manhattan Study.** *Circulation* 2005;111:1327–31 [CrossRef Medline](#)
3. Wong KS, Huang YN, Gao S, et al. **Intracranial stenosis in Chinese patients with acute stroke.** *Neurology* 1998;50:812–13 [CrossRef Medline](#)
4. de Havenon A, Mossa-Basha M, Shah L, et al. **High-resolution vessel wall MRI for the evaluation of intracranial atherosclerotic disease.** *Neuroradiology* 2017;59:1193–202 [CrossRef Medline](#)
5. Mossa-Basha M, Alexander M, Gaddikeri S, et al. **Vessel wall imaging for intracranial vascular disease evaluation.** *J Neurointerv Surg* 2016;8:1154–59 [CrossRef Medline](#)
6. Alexander MD, de Havenon A, Kim SE, et al. **Assessment of quantitative methods for enhancement measurement on vessel wall magnetic resonance imaging evaluation of intracranial atherosclerosis.** *Neuroradiology* 2019;61:643–50 [CrossRef Medline](#)
7. Dieleman N, Yang W, Abrigo JM, et al. **Magnetic resonance imaging of plaque morphology, burden, and distribution in patients with symptomatic middle cerebral artery stenosis.** *Stroke* 2016;47:1797–802 [CrossRef Medline](#)
8. Gorelick PB, Wong KS, Bae HJ, et al. **Large artery intracranial occlusive disease: a large worldwide burden but a relatively neglected frontier.** *Stroke* 2008;39:2396–99 [CrossRef Medline](#)
9. Portanova A, Hakakian N, Mikulis DJ, et al. **Intracranial vasa vasorum: insights and implications for imaging.** *Radiology* 2013;267:667–79 [CrossRef Medline](#)
10. Qiao Y, Zeiler SR, Mirbagheri S, et al. **Intracranial plaque enhancement in patients with cerebrovascular events on high-spatial-resolution MR images.** *Radiology* 2014;271:534–42 [CrossRef Medline](#)
11. Wang E, Shao S, Li S, et al. **A high-resolution MRI study of the relationship between plaque enhancement and ischemic stroke events in patients with intracranial atherosclerotic stenosis.** *Front Neurol* 2018;9:1154 [CrossRef Medline](#)
12. Kim JM, Jung KH, Sohn CH, et al. **Intracranial plaque enhancement from high resolution vessel wall magnetic resonance imaging predicts stroke recurrence.** *Int J Stroke* 2016;11:171–79 [CrossRef Medline](#)
13. Song X, Zhao X, Liebeskind DS, et al. **Incremental value of plaque enhancement in predicting stroke recurrence in symptomatic intracranial atherosclerosis.** *Neuroradiology* 2020;62:1123–31 [CrossRef Medline](#)
14. Yang D, Liu J, Yao W, et al. **The MRI enhancement ratio and plaque steepness may be more accurate for predicting recurrent ischemic**

- cerebrovascular events in patients with intracranial atherosclerosis. *Eur Radiology* 2022;32:7004–13 [CrossRef Medline](#)
15. Xu C, Qin J, Yu J, et al. Association of plaque enhancement on vessel wall MRI and the phosphodiesterase 4D variant with stroke recurrence in patients with symptomatic intracranial atherosclerosis. *Neuroradiology* 2022;64:1781–94 [CrossRef Medline](#)
 16. van der Kolk AG, Zwanenburg JJ, Brundel M, et al. Intracranial vessel wall imaging at 7.0-T MRI. *Stroke* 2011;42:2478–84 [CrossRef Medline](#)
 17. Lu SS, Ge S, Su CQ, et al. MRI of plaque characteristics and relationship with downstream perfusion and cerebral infarction in patients with symptomatic middle cerebral artery stenosis. *J Magn Reson Imaging* 2018;48:66–73 [CrossRef Medline](#)
 18. Li X, Sun B, Wang L, et al. Association of type 2 diabetes mellitus and glycemic control with intracranial plaque characteristics in patients with acute ischemic stroke. *J Magn Reson Imaging* 2021;54:655–66 [CrossRef Medline](#)
 19. Song JW, Pavlou A, Burke MP, et al. Imaging endpoints of intracranial atherosclerosis using vessel wall MR imaging: a systematic review. *Neuroradiology* 2021;63:847–56 [CrossRef Medline](#)
 20. Shi Z, Li J, Zhao M, et al. Quantitative histogram analysis on intracranial atherosclerotic plaques: a high-resolution magnetic resonance imaging study. *Stroke* 2020;51:2161–69 [CrossRef Medline](#)
 21. Wu G, Wang H, Zhao C, et al. Large culprit plaque and more intracranial plaques are associated with recurrent stroke: a case-control study using vessel wall imaging. *AJNR Am J Neuroradiol* 2022;43:207–15 [CrossRef Medline](#)
 22. Ran Y, Wang Y, Zhu M, et al. Higher plaque burden of middle cerebral artery is associated with recurrent ischemic stroke: a quantitative magnetic resonance imaging study. *Stroke* 2020;51:659–62 [CrossRef Medline](#)
 23. Sun B, Wang L, Li X, et al. Intracranial atherosclerotic plaque characteristics and burden associated with recurrent acute stroke: a 3D quantitative vessel wall MRI study. *Front Aging Neurosci* 2021;13:706544 [CrossRef Medline](#)
 24. Wu F, Ma Q, Song H, et al. Differential features of culprit intracranial atherosclerotic lesions: a whole-brain vessel wall imaging study in patients with acute ischemic stroke. *J Am Heart Assoc* 2018;7:e009705
 25. Vakil P, Vranic J, Hurley MC, et al. T1 gadolinium enhancement of intracranial atherosclerotic plaques associated with symptomatic ischemic presentations. *AJNR Am J Neuroradiol* 2013;34:2252–58 [CrossRef Medline](#)
 26. Skarpathiotakis M, Mandell DM, Swartz RH, et al. Intracranial atherosclerotic plaque enhancement in patients with ischemic stroke. *AJNR Am J Neuroradiol* 2013;34:299–304 [CrossRef Medline](#)
 27. Wang W, Yang Q, Li D, et al. Incremental value of plaque enhancement in patients with moderate or severe basilar artery stenosis: 3.0 T high-resolution magnetic resonance study. *Biomed Res Int* 2017;2017:4281629 [CrossRef Medline](#)
 28. Vakil P, Elmokadem AH, Syed FH, et al. Quantifying intracranial plaque permeability with dynamic contrast-enhanced MRI: a pilot study. *AJNR Am J Neuroradiol* 2017;38:243–49 [CrossRef Medline](#)
 29. Ntaios G, Pearce LA, Meseguer E, et al. Aortic arch atherosclerosis in patients with embolic stroke of undetermined source: an exploratory analysis of the NAVIGATE ESUS trial. *Stroke* 2019;50:3184–90 [CrossRef Medline](#)
 30. Wang J, Yarnykh VL, Yuan C. Enhanced image quality in black-blood MRI using the improved motion-sensitized driven-equilibrium (iMSDE) sequence. *J Magn Reson Imaging* 2010;31:1256–63 [CrossRef Medline](#)
 31. Wang J, Zhang S, Lu J, et al. High-resolution MR for follow-up of intracranial steno-occlusive disease treated by endovascular treatment. *Front Neurol* 2021;12:706645 [CrossRef Medline](#)
 32. Hartman JB, Watase H, Sun J, et al. Intracranial aneurysms at higher clinical risk for rupture demonstrate increased wall enhancement and thinning on multicontrast 3D vessel wall MRI. *Br J Radiology* 2019;92:20180950 [CrossRef Medline](#)
 33. de Havenon A, Muhina HJ, Parker DL, et al. Effect of time elapsed since gadolinium administration on atherosclerotic plaque enhancement in clinical vessel wall MR imaging studies. *AJNR Am J Neuroradiol* 2019;40:1709–11 [CrossRef Medline](#)
 34. Szolar DH, Korobkin M, Reittner P, et al. Adrenocortical carcinomas and adrenal pheochromocytomas: mass and enhancement loss evaluation at delayed contrast-enhanced CT. *Radiology* 2005;234:479–85 [CrossRef Medline](#)
 35. Kwee RM, Qiao Y, Liu L, et al. Temporal course and implications of intracranial atherosclerotic plaque enhancement on high-resolution vessel wall MRI. *Neuroradiology* 2019;61:651–57 [CrossRef Medline](#)